JOURNAL OF MATERIALS SCIENCE 22 (1987) 1827–1834

Microstructure and superconducting properties of rapidly-quenched copper-based alloys containing immiscible lead and bismuth elements

AKIHISA INOUE, NOBUYOSHI YANO*, KUNIO MATSUZAKI, TSUYOSHI MASUMOTO
The Research Institute for Iron, Steel and Other Metals, Tohoku University, Sendai 980, Japan

Copper-based superconducting alloys including finely dispersed fcc lead or hcp ε(Pb–Bi) particles in fcc copper matrix have been obtained by rapid quenching $(Cu–M)_{100-x}Pb_x$ and $(Cu–M)_{100-x}(Pb_{0.6}Bi_{0.4})_x$ (M = aluminium, silicon or tin; $x \leqslant 10$ at%) alloys containing immiscible elements such as lead and bismuth. The particle size and interparticle distance were about 30 to 130 nm and 20 to 200 nm for lead particles and about 30 to 60 nm and 30 to 150 nm for ε(Pb–Bi) particles. The transition temperature, T_c, was in the range of 3.2 to 5.5 K for the Cu–M–Pb alloys and 6.2 to 6.3 K for the Cu–M–Pb–Bi alloys. Critical magnetic field, H_{c2}, and critical current density, J_c, for the latter alloys were 0.47 to 0.93 T at 4.2 K and 1.1×10^5 to 2.7×10^5 Am^{-2} at zero applied field and 4.21 K. The mechanism of the appearance of such a soft-type superconductivity for the rapidly quenched copper-based alloys was discussed, and inferred to be due to the formation of a percolation path of a superconducting lead or Pb–Bi phase along the grain boundaries, sub-boundaries and/or tangled dislocations where the lead or Pb–Bi phase precipitated preferentially, rather than the proximity effect based on lead or Pb–Bi particles.

1. Introduction

Most of the investigations [1] on rapidly solidified alloys which have been carried out to date have focussed on the formation and characterization on nonequilibrium phases in alloys around eutectic and intermetallic compound compositions. This focalization is probably due to the good possibility of nonequilibrium phase formation due to greater supercooling capacity and strong attractive interaction between the constituent elements. However, the present authors have very recently demonstrated for a number of alloys of nickel- [2], copper- [3], iron- [4], cobalt- [4], aluminium- [5], germanium- [6] and Al–O oxide- [7] based systems, that application of rapid quenching to alloys with the element exhibiting a large liquidus miscibility gap against major constituent elements results in the formation of a new type of duplex structure. This structure consists of an amorphous phase or a supersaturated solid solution including finely and densely dispersed immiscible metal particles. Furthermore, the duplex alloys have been found [2–7] to exhibit useful functional properties such as improved superconductivity, large electrical resistivity combined with large positive temperature dependence, large magnetoresistivity, etc., which are not obtainable for the single phase alloys. The present study is one of a series of investigations on rapid solidification of alloys with a large miscibility gap, and our aim is to clarify whether or not copper-based crystalline alloys with finely dispersed immiscible lead or lead + bismuth particles are formed by the rapid-quenching technique and whether the duplex alloys exhibit a good superconductivity in the rapidly quenched state.

2. Experimental procedure

Alloys with different compositions $(Cu_{0.94}Al_{0.06})_{100-x}Pb_x$, $(Cu_{0.9}Si_{0.1})_{100-x}Pb_x$, $(Cu_{0.95}Sn_{0.05})_{100-x}Pb_x$ ($x \leqslant 10$ at%), $(Cu_{0.94}Al_{0.06})_{98}Pb_{1.2}Bi_{0.8}$, $(Cu_{0.9}Si_{0.1})_{98}Pb_{1.2}Bi_{0.8}$ and $(Cu_{0.95}Sn_{0.05})_{98}Pb_{1.2}Bi_{0.8}$ were used in the present work. The concentrations of aluminium, silicon and tin are almost equal to those of solid solubility limit at room temperature in the equilibrium phase diagrams of Cu–Al, Cu–Si and Cu–Sn [8]. The alloy ingots were prepared by arc melting the mixture of the prealloyed Cu–Al, Cu–Si or Cu–Sn ingot and pure lead and/or bismuth metals in a purified argon atmosphere. Typically, the amount of each ingot melted in one arc melting was about 3 g and the whole ingot was used in one rapid-quenching operation to produce ribbon samples of about 2 mm width and 0.03 mm thickness in air by a single-roller spinning apparatus with a copper wheel. Compositions of the alloys are nominal, since the loss of lead during melting was usually below 0.3 wt %. The as-quenched structure was examined by

* *Permanent address*: Unitika Research and Development Center, Unitika Ltd., Uji 611, Japan.

0022–2461/87 $03.00 + .12

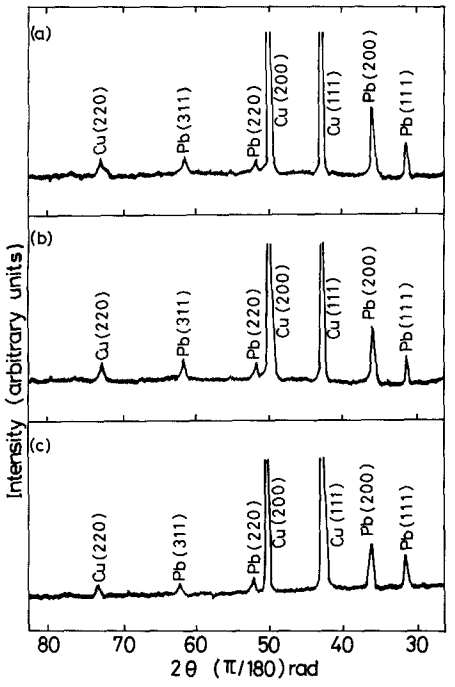

Figure 1 X-ray diffraction patterns showing the duplex structure consisting of copper phase containing aluminium, silicon or tin and fcc lead phase in rapidly quenched (a) $(Cu_{0.95}Al_{0.05})_{98}Pb_2$ (b) $(Cu_{0.9}Si_{0.1})_{98}Pb_2$ and (c) $(Cu_{0.95}Sn_{0.05})_{98}Pb_2$ alloys.

X-ray diffractometry and optical and transmission electron microscopy. Measurements of superconducting properties, transition temperature, T_c, critical current density, J_c (H), critical magnetic field, H_c, H_{c2} (T) and flux flow resistivity, ϱ_f (H) were made by the DC method using the four electrical probes. The temperature was measured with an accuracy of ± 0.01 K using a calibrated germanium thermometer. The magnetic field up to 9 T was applied perpendicularly to the specimen surface and feed current.

3. Results

3.1. Rapidly quenched structure

Fig. 1 shows the X-ray diffraction patterns of rapidly quenched $(Cu_{0.95}Al_{0.05})_{98}Pb_2$, $(Cu_{0.95}Si_{0.05})_{98}Pb_2$ and $(Cu_{0.95}Sn_{0.05})_{98}Pb_2$ alloys. Some weak diffraction peaks corresponding to fcc lead are seen, in addition to the diffraction peaks of copper with high intensities, indicating the formation of a coexistent structure of fcc copper and fcc lead phases. The lattice parameters of copper and lead are 0.3634 and 0.4955 nm, respectively, for the Cu–Al–Pb alloy, 0.3619 and 0.4954 nm for the Cu–Si–Pb alloy, and 0.3660 and 0.4951 nm for the Cu–Sn–Pb alloy. The actually measured lattice parameters of lead are nearly equal to that (0.49502 nm) [9] of pure lead, whereas the lattice parameters of copper phase are larger than that (0.36147 nm) [9] of pure copper by about 0.5% for the Cu–Al–Pb alloy, about 0.4% for the Cu–Si–Pb alloy and about 1.3% for the Cu–Sn–Pb alloy. From the data of the lattice parameters, one can derive the following results: (i) copper and aluminium, silicon or tin elements are immiscible against the lead phase, and (ii) the lattice parameters of the copper phase in the Cu–M–Pb (M = aluminium, silicon or tin) alloys agree with those of copper solid solution containing about 8 at % Al, 5.9 at % Si or 7.7 at % Sn [9], and it is therefore thought that aluminium, silicon or tin dissolved preferentially into copper rather than lead. The distribution of each constituent element into two phases is consistent with the expectation from the equilibrium phase diagrams of Cu–Pb, Cu–M and Pb–M [8] binary alloys.

Fig. 2 shows typical transmission electron micrographs revealing distribution of an immiscible lead phase in rapidly quenched $(Cu_{0.95}Al_{0.05})_{99}Pb_1$ and $(Cu_{0.95}Al_{0.05})_{98}Pb_2$ alloys. As seen in the photographs, the distribution of lead particles appears very homogeneous within the inner area of each grain, but there is a preferential precipitation of lead particles on the grain boundaries and sub-boundaries in the copper matrix. The average particle diameter and interparticle distance of the lead phase within the grains were estimated to be, respectively, 50 to 100 and 100 to 500 nm for $(Cu_{0.95}Al_{0.05})_{99}Pb_1$; 30 to 90 and 20 to 150 nm for $(Cu_{0.95}Al_{0.05})_{98}Pb_2$; 70 to 130 and 40 to 150 nm for $(Cu_{0.95}Al_{0.05})_{96}Pb_4$; 40 to 80 and 90 to 450 nm for $(Cu_{0.95}Si_{0.05})_{99}Pb_1$; 30 to 70 and 50 to 200 nm for $(Cu_{0.95}Si_{0.05})_{98}Pb_2$; 50 to 120 and 100 to 500 nm for $(Cu_{0.95}Sn_{0.05})_{99}Pb_1$; and 40 to 100 and 40 to 130 nm for $(Cu_{0.95}Sn_{0.05})_{98}Pb_2$. The particle size on the grain boundaries and sub-boundaries is nearly the same as those within the grains, but the interparticle distance is much smaller and in many cases the particles appear to connect directly with each other.

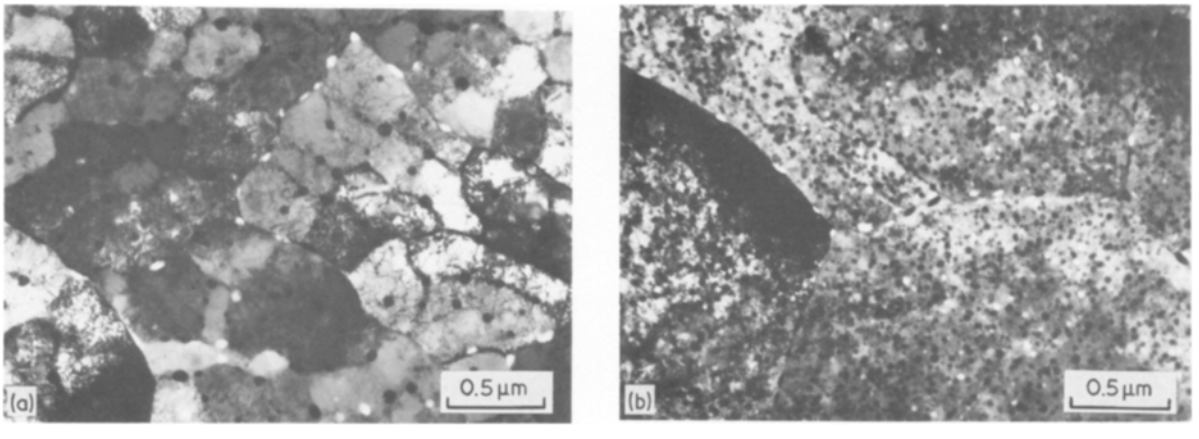

Figure 2 Transmission electron micrographs showing the duplex microstructure consisting of a copper matrix containing aluminium and fcc lead phase in rapidly quenched (a) $(Cu_{0.95}Al_{0.05})_{99}Pb_1$ and (b) $(Cu_{0.95}Al_{0.05})_{98}Pb_2$ alloys.

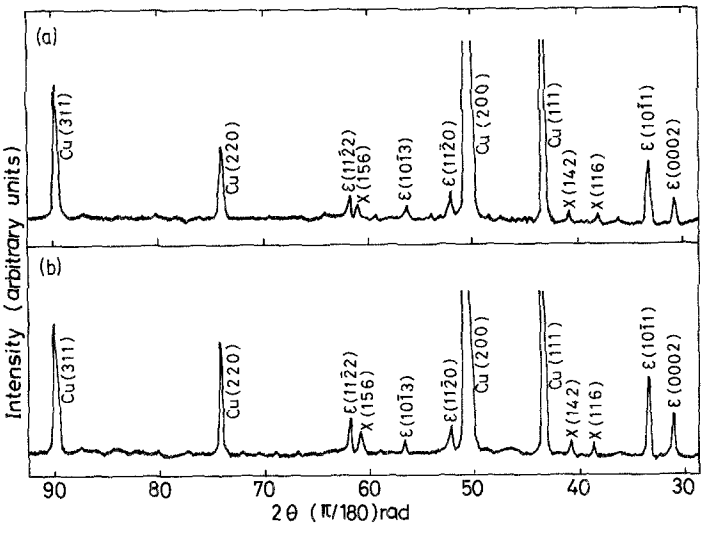

Figure 3 X-ray diffraction patterns showing the mixed structure consisting of copper phase containing silicon, hcp ε(Pb–Bi) and bct X(Pb–Bi) phases in rapidly quenched (a) $(Cu_{0.95}Al_{0.05})_{98}Pb_{1.2}Bi_{0.8}$ and (b) $(Cu_{0.9}Si_{0.1})_{98}Pb_{1.2}Bi_{0.8}$ alloys.

A similar coexistent structure of copper and immiscible second phase was also obtained for $(Cu_{0.95}Al_{0.05})_{98}Pb_{1.2}Bi_{0.8}$ and $(Cu_{0.9}Si_{0.1})_{98}Pb_{1.2}Bi_{0.8}$ alloys as seen in Figs 3 and 4. Precipitates in the alloys containing both lead and bismuth can be identified to consist of two phases of an hcp ε-phase with $a \simeq 0.350$ nm and $c \simeq 0.580$ nm and a bct X-phase with $a \simeq 0.993$ nm and $c \simeq 1.449$ nm. The ε phase is a supersaturated solid solution of an equilibrium hcp phase which exists in the range of 24 to 33 at % Bi at room temperature [10, 11] and the X phase is a nonequilibrium phase which appears only in a rapidly solidified case [12]. Considering the result that the lattice parameters of ε and X phases in the rapidly quenched Cu–Si–Pb–Bi alloy agree with those [10–12] of Pb–Bi binary alloys, it is inferred that the ε and X precipitates do not dissolve an appreciable amount of copper and silicon. This inference is also consistent with the result that the lattice parameter of copper matrix in rapidly quenched $(Cu_{0.9}Si_{0.1})_{98}Pb_{1.2}Bi_{0.8}$ alloy is 0.3621 nm which is nearly equal to that of $Cu_{90.4}Si_{9.6}$ solid solution [9]. The particle diameter and interparticle distance of dispersed ε and X phases are about 30 to 60 and 30 to 150 nm, respectively, being almost the same order as those of lead particles in Cu–Al, Cu–Si and Cu–Sn matrices. Here it appears important from an engineering point of view to point out that all the copper-based alloy ribbons containing immiscible particles possess a good bending ductility which is shown by 180° bending. Formation of the ductile copper-phase alloys with homogeneously dispersed lead or lead–bismuth particles was limited to the compositions less than about 5 at % Pb for $(Cu_{0.95}M_{0.05})_{100-x}Pb_x$ (M = aluminium, silicon or tin) and about 5 at % (Pb + Bi) for $(Cu_{0.9}Si_{0.1})_{100-x}(Pb_{0.6}Bi_{0.4})_x$. A further increase in the additional amount of lead and bismuth resulted in the formation of macroscopically inhomogeneous ribbon samples consisting of the duplex copper-based phase with dispersed lead or lead–bismuth particles and pure lead or the pure ε + bismuth phase itself.

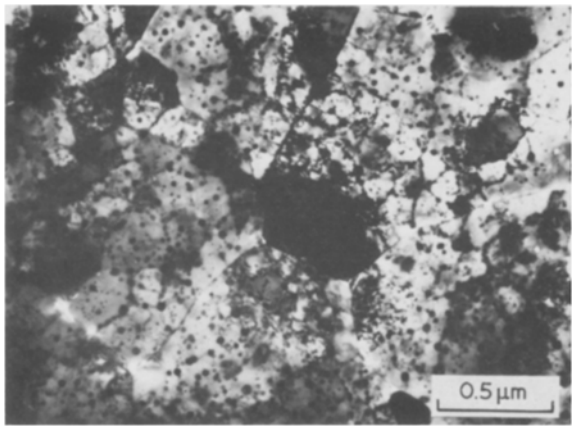

Figure 4 Transmission electron micrograph showing the mixed structure consisting of copper phase containing silicon, hcp ε(Pb–Bi) and bct X(Pb–Bi) phases in a rapidly quenched $(Cu_{0.9}Si_{0.1})_{98}Pb_{1.2}Bi_{0.8}$ alloy.

3.2. Superconducting properties

Typical examples of the normalized electrical resistance (R/R_n) curves in the vicinity of T_c in the case of no applied magnetic field are shown in Fig. 5 for $(Cu_{0.95}Al_{0.05})_{98}Pb_2$, $(Cu_{0.95}Al_{0.05})_{96}Pb_4$, $(Cu_{0.95}Si_{0.05})_{98}Pb_2$, $(Cu_{0.95}Si_{0.05})_{96}Pb_4$, $(Cu_{0.95}Sn_{0.05})_{98}Pb_2$ and $(Cu_{0.95}Sn_{0.05})_{96}Pb_4$, and in Fig. 6 for $(Cu_{0.95}Al_{0.05})_{98}Pb_{1.2}Bi_{0.8}$, $(Cu_{0.95}Al_{0.05})_{96}Pb_{2.4}Bi_{1.6}$, $(Cu_{0.9}Si_{0.1})_{98}Pb_{1.2}Bi_{0.8}$ and $(Cu_{0.9}Si_{0.1})_{96}Pb_{2.4}Bi_{1.6}$. Additionally, the data of $(Al_{0.9}Si_{0.1})_{98}Pb_2$ and $(Al_{0.9}Si_{0.1})_{98}Pb_{1.2}Bi_{0.8}$ alloys are presented in Figs 5 and 6 for comparison. Here R_n is the resistance in the normal state. The transition occurs rather broadly with a temperature width (ΔT_c) ranging from 1.2 to 2.2 K. The transition temperature T_c, which was taken as the temperature at $R/R_n = 0.5$, is 3.6 K at 2% Pb and 5.3 K at 4% Pb for the Cu–Al–Pb alloys, 3.2 K at 2% Pb and 4.3 K at 4% Pb for the Cu–Si–Pb alloys, 3.8 K at 2% Pb and 5.5 K at 4% Pb for the Cu–Sn–Pb alloys, 6.2 K for the Cu–Si–Pb–Bi alloy and 6.3 K for the Cu–Al–Pb–Bi alloy. From these data, the following conclusions may be derived:

1. T_c decreases in the order of Cu–Al–Pb–Bi > Cu–Si–Pb–Bi > Cu–Sn–Pb > Cu–Al–Pb > Cu–Si–Pb. Thus T_c of the alloys containing lead and bismuth is higher by about 0.9 to 2.9 K than that of the alloys containing only lead.

2. The increase in lead content from 2 to 4% results in a rise of T_c by about 1.1 to 1.7 K.

3. T_c of the lead-containing alloys is almost the same between Cu–Si–Pb and Al–Si–Pb, but that of

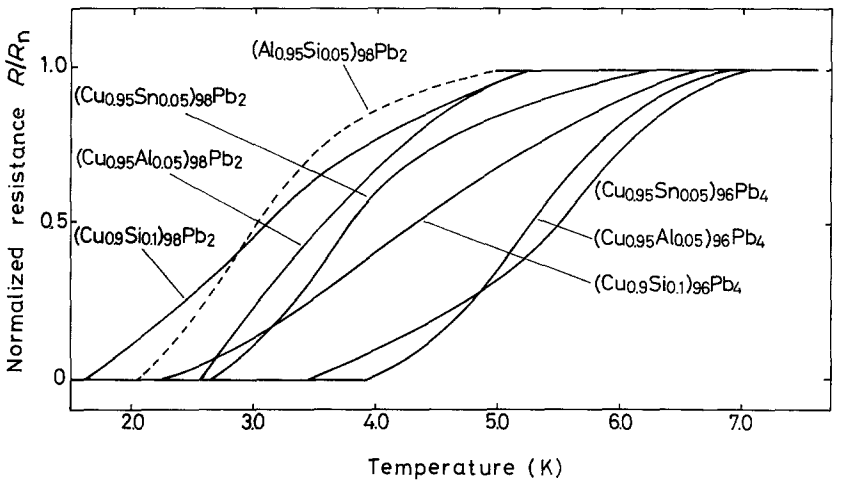

Figure 5 Normalized resistance ratio R/R_n as a function of temperature for rapidly quenched $(Cu_{0.95}Al_{0.05})_{100-x}Pb_x$, $(Cu_{0.9}Si_{0.1})_{100-x}Pb_x$ and $(Cu_{0.95}Sn_{0.05})_{100-x}Pb_x$ (x = 2 and 4 at %) alloys possessing the coexistent Cu(Al) and lead phases. The result of a rapidly quenched $(Al_{0.95}Si_{0.05})_{98}Pb_2$ alloy is also shown for comparison.

the alloys containing both lead and bismuth is much higher for Al–Si–Pb–Bi than for Cu–Al–Pb–Bi and Cu–Si–Pb–Bi.

4. ΔT_c of the copper-based alloys are larger by about 0.05 to 0.3 K than those of the aluminium-based alloys.

The critical magnetic field, H_c, was measured at various temperatures ranging from 1.5 to T_c. The temperature dependence of H_c and H_{c2} is shown in Fig. 7 for $(Cu_{0.95}Al_{0.05})_{98}Pb_2$ and $(Cu_{0.95}Al_{0.05})_{96}Pb_4$ and in Fig. 8 for $(Cu_{0.9}Si_{0.1})_{98}Pb_{1.2}Bi_{0.8}$ and $(Cu_{0.95}Al_{0.05})_{98}Pb_{1.2}Bi_{0.8}$, where the solid lines represent a linear extrapolation at T_c. Here we define H_c and H_{c2} to be the applied magnetic field at which the resistance of the samples begins to appear. H_c increases linearly with lowering temperature over almost the whole temperature range and the gradient at T_c, $-(dH_{c2}/dT)_{T_c}$, is $1.7 \times 10^{-2}\,TK^{-1}$ for the Cu–Al–2Pb alloy, $1.9 \times 10^{-2}\,TK^{-1}$ for the Cu–Al–4Pb alloy, $0.30\,TK^{-1}$ for the Cu–Al–Pb–Bi alloy and $0.23\,TK^{-1}$ for the Cu–Si–Pb–Bi alloy. It is thus noticed that the gradient of the alloys containing lead and bismuth is about 12 to 18 times higher than that of the lead-containing alloy through the difference in the type of their superconductors, i.e., type I for lead and type II for lead–bismuth [13]. As expected from the marked difference in the gradient, the critical field at 2.0 K is 0.027 T for Cu–Al–2Pb and 0.066 T for Cu–Al–4Pb which are much lower than those (0.91 to 1.42 T) for the Cu–Al–Pb–Bi and Cu–Si–Pb–Bi alloys.

The critical current density, J_c, was measured at 4.21 and 1.40 K under an external applied magnetic field for $(Cu_{0.95}Al_{0.05})_{98}Pb_{1.2}Bi_{0.8}$ and $(Cu_{0.95}Si_{0.05})_{98}Pb_{1.2}Bi_{0.8}$ alloys exhibiting high T_c among all the alloys examined in the present work. J_c as a function of external applied field is plotted in Fig. 9. The value of J_c in the absence of applied field is about $2.7 \times 10^5\,Am^{-2}$ at 4.21 K and $1.4 \times 10^7\,Am^{-2}$ at 1.40 K for the Cu–Al–Pb–Bi alloy and about $1.1 \times 10^5\,Am^{-2}$ at 4.21 K and $4.6 \times 10^6\,Am^{-2}$ at 1.40 K for the Cu–Si–Pb–Bi alloy, and the value decreases rapidly with increasing applied field. For example, at $H = 0.3$ T, J_c is about $3.6 \times 10^4\,Am^{-2}$ at 4.21 K and $2.4 \times 10^5\,Am^{-2}$ at 1.40 K for the former alloy, and $4.0 \times 10^3\,Am^{-2}$ at 4.21 K and $1.0 \times 10^5\,Am^{-2}$ at 1.40 K for the latter alloy.

The fluxoid pinning force F_p evaluated from Fig. 9 is plotted as a function of reduced magnetic field H/H_{c2} in Fig. 10, where F_p is calculated as $J_c \times H$. The maximum F_p and the value of H/H_{c2} where F_p shows a maximum value are, respectively, $3.9 \times 10^3\,Nm^{-3}$ and 0.30 at 4.21 K and $9 \times 10^4\,Nm^{-3}$ and 0.10 at 1.40 K for the Cu–Si–Pb–Bi alloy and $1.1 \times 10^4\,Nm^{-3}$ and 0.28 at 4.21 K and $1.5 \times 10^5\,Nm^{-3}$ and 0.03 at 1.40 K for the Cu–Al–Pb–Bi alloy.

4. Discussion

In this section, the mechanism for the appearance of superconductivity for copper-based alloys possessing the coexistent copper-based solid solution and f c c lead or h c p ε(Pb–Bi) + b c t X(Pb–Bi) will firstly be discussed. Copper-based solid solutions dissolving a

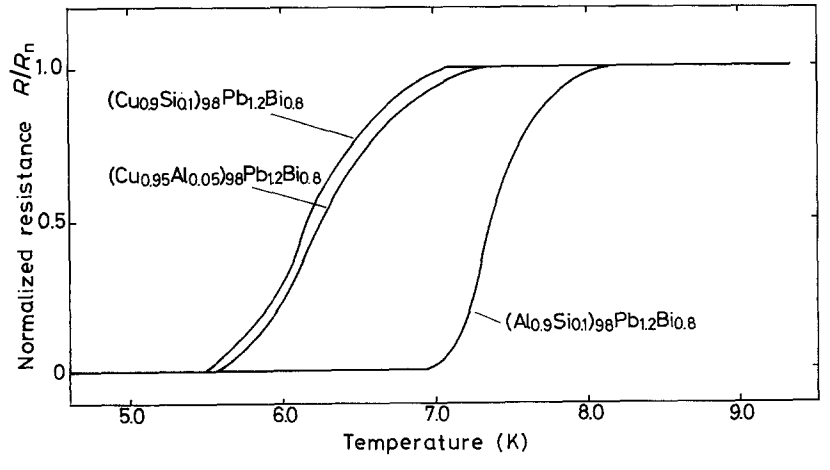

Figure 6 Normalized resistance ratio R/R_n as a function of temperature for rapidly quenched $(Cu_{0.95}Al_{0.05})_{100-x}(Pb_{0.6}Bi_{0.4})_x$ and $(Cu_{0.9}Si_{0.1})_{100-x}(Pb_{0.6}Bi_{0.4})_x$ (x = 2 and 4 at %) alloys possessing the coexistent Cu(Si or Sn), h c p ε(Pb–Bi) and b c t X(Pb–Bi) phases. The result of a rapidly quenched $(Al_{0.9}Si_{0.1})_{98}Pb_{1.2}Bi_{0.8}$ alloy is also shown for comparison.

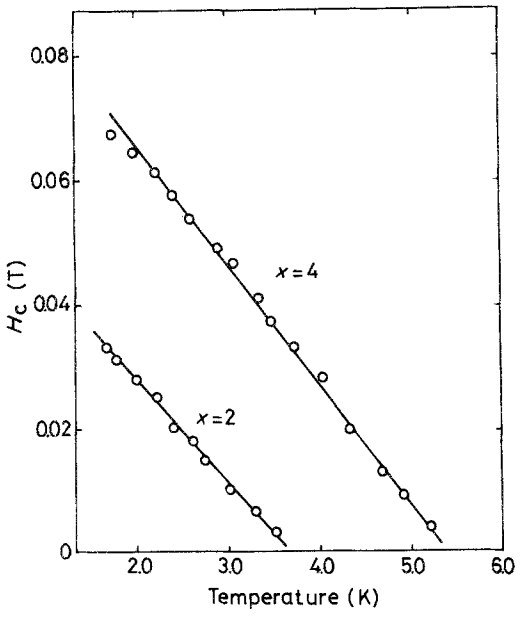

Figure 7 The critical magnetic field (H_c) at various temperatures for rapidly quenched $(Cu_{0.95}Al_{0.05})_{100-x}Pb_x$ (x = 2 and 4 at %) alloys possessing the coexistent Cu(Al) and lead phases. The solid line represents a linear extrapolation near T_c.

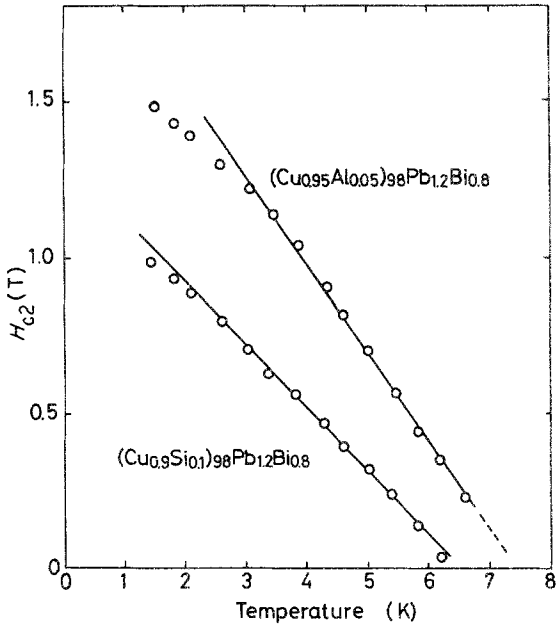

Figure 8 The upper critical magnetic field (H_{c2}) at various temperatures for rapidly quenched $(Cu_{0.95}Al_{0.05})_{98}Pb_{1.2}Bi_{0.8}$ and $(Cu_{0.9}Si_{0.1})_{98}Pb_{1.2}Bi_{0.8}$ alloys possessing the coexistent Cu(Al or Si), ε(Pb–Bi) and X(Pb–Bi) phases.

small amount of aluminium, silicon or tin are non-superconductive. Accordingly, the present appearance of superconductivity for the copper-based alloys containing lead or ε(Pb–Bi) + X(Pb–Bi) particles is thought to originate from one of the following three mechanisms: (i) formation of a surface thin layer of superconducting lead or lead–bismuth phase, (ii) formation of a percolation path of lead or lead–bismuth phase, and (iii) the proximity effect due to lead or lead–bismuth particles. The present superconductivity was confirmed to remain almost unchanged even after reduction of the sample thickness by about 20%, by any method of chemical, electrical or mechanical polishing. It is therefore unreasonable to infer that the appearance of superconductivity for the present copper-based alloys is due to the formation of a surface thin layer consisting of a lead or lead–bismuth phase with superconductivity.

Secondarily, the proximity effect resulting from lead or lead–bismuth superconducting particles is discussed as a mechanism for the superconductivity of the copper-based alloys, Table I summarizes the nominal composition, T_c and residual electrical resistivity of some rapidly quenched alloys and the particle diameter ($2r$) and interparticle distance (D) of lead and lead–bismuth phases, together with the data [5] for similar aluminium-based alloys prepared by rapid quenching. From the residual electrical resistivities of about 0.05 to 0.15 $\mu\Omega$m, the mean free path of electrons (l) is estimated to be of the order 3.4×10^{-4} to 1.0×10^{-3} m for the copper-based alloys from the nearly free electron model [14]. Further, the coherence length (ξ_0) of the copper-based matrix has reasonably been inferred to be smaller than 1000 nm from the data of superconducting pure metals of aluminium, niobium,

TABLE I Comparison of properties of rapidly quenched Cu–M–Pb (M = aluminium, silicon or tin) and Cu–M–Pb–Bi (M = aluminium or silicon) alloys possessing the coexistent Cu(Al, Si or Sn) and lead or hcp ε(Pb–Bi) + bct X(Pb–Bi) phases with reference to rapidly quenched Al–Pb, Al–Si–Pb and Al–Si–Pb–Bi alloys consisting of aluminium and lead or ε(Pb–Bi) taken from [5]: particle size ($2r$) and interparticle distance (D) of lead or hcp ε(Pb–Bi) and/or bct X(Pb–Bi) phases embedded in copper matrix, superconducting transition temperature (T_c), upper critical field gradient at T_c, $-(dH_{c2}/dT)_{T_c}$, upper critical field (H_{c2}) at 2.0 K, the residual electrical resistivity (ϱ_n) and the ratio of particle radius against the coherence length of lead or ε(Pb–Bi) (r/ξ_0^*).

Alloy (at %)	$2r$ (nm)	D (nm)	T_c (K)	$-(dH_{c2}/dT)_{T_c}$ (T/K)	H_{c2} at 2.0 K (T)	ϱ_n ($\mu\Omega$m)	r/ξ_0^*
$(Cu_{0.95}Al_{0.05})_{98}Pb_2$	30–90	20–150	3.6	0.017	0.027	0.0018	0.18–0.54
$(Cu_{0.95}Al_{0.05})_{96}Pb_4$	70–130	40–150	5.3	0.019	0.066	0.0027	0.42–0.78
$(Cu_{0.9}Si_{0.1})_{98}Pb_2$	30–70	50–200	3.2	–	–	–	0.18–0.42
$(Cu_{0.9}Si_{0.1})_{96}Pb_4$	50–100	80–200	4.3	–	–	–	0.30–0.60
$(Cu_{0.95}Sn_{0.05})_{98}Pb_2$	40–100	40–130	3.8	–	–	–	0.24–0.60
$(Cu_{0.95}Sn_{0.05})_{96}Pb_4$	–	–	5.5	–	–	–	–
$(Cu_{0.95}Al_{0.05})_{98}Pb_{1.2}Bi_{0.8}$	30–60	20–150	6.3	0.30	1.41	0.085	0.65–1.30
$(Cu_{0.9}Si_{0.1})_{98}Pb_{1.2}Bi_{0.8}$	30–50	20–200	6.2	0.23	0.91	0.13	0.65–1.09
$Al_{98}Pb_2$	40	40–100	4.16	–	–	0.0027	0.24
$(Al_{0.9}Si_{0.1})_{98}Pb_2$	40	30–100	2.94	–	–	–	0.24
$(Al_{0.9}Si_{0.1})_{98}Pb_{1.2}Bi_{0.8}$	20–40	20–70	7.38	0.070	0.196 at 4.2 K	0.14	0.43–0.87
$(Al_{0.9}Si_{0.1})_{95}Pb_3Bi_2$	15–60	30–60	7.75	0.075	0.212 at 4.2 K	0.16	0.33–1.30

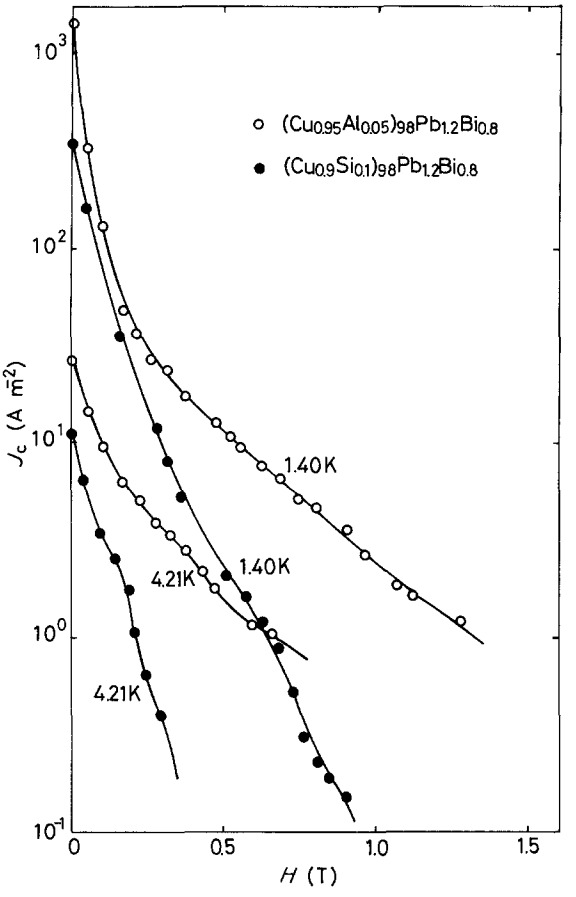

Figure 9 Critical current density (J_c) as a function of magnetic field for rapidly quenched $(Cu_{0.95}Al_{0.05})_{98}Pb_{1.2}Bi_{0.8}$ and $(Cu_{0.9}Si_{0.1})_{98}Pb_{1.2}Bi_{0.8}$ alloys possessing the coexistent Cu(Al or Si), ε(Pb–Bi) and X(Pb–Bi) phases.

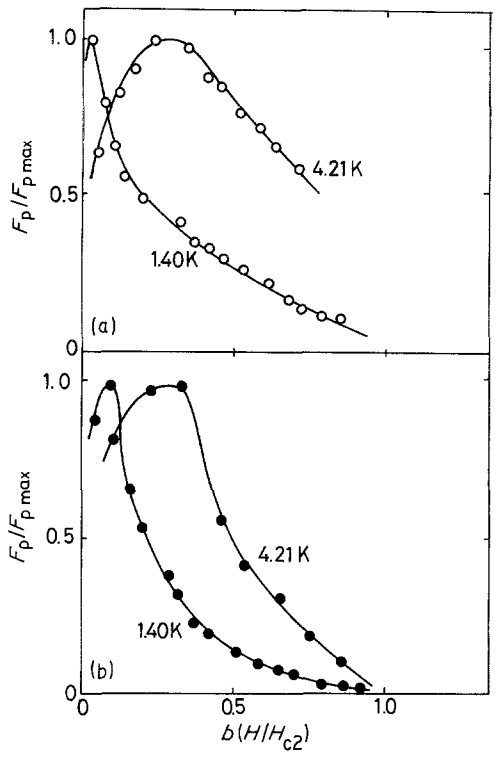

Figure 10 Fluxoid pinning force F_p as a function of reduced magnetic field H/H_{c2} for rapidly quenched (a) $(Cu_{0.95}Al_{0.05})_{98}Pb_{1.2}Bi_{0.8}$ and (b) $(Cu_{0.9}Si_{0.1})_{98}Pb_{1.2}Bi_{0.8}$ alloys possessing the coexistent Cu(Al or Si), ε(Pb–Bi) and X(Pb–Bi) phases. $F_{p,max}$ = (a) 1.40 K, 15 Nm^{-3}; 4.21 K, 1.1 Nm^{-3}, (b) 1.40 K, 9 Nm^{-3}; 4.21 K, 0.39 Nm^{-3}.

lead, tin etc. The superconductivity caused by the proximity effect has been considered to be dominated by the characteristics of the matrix phase [15] and the present alloys consisting of copper-based solid solution and lead or lead–bismuth phases can be classified as typical of clean superconductors, since $l \gg \xi_0$ for the copper-based matrix.

The leak distance (K_n^{-1}) for the proximity effect in the case of clean limit is given by the following relation [15]

$$K_n^{-1} = hv_n/2\pi k_B T \quad (1)$$

where v_n is the Fermi velocity of electrons in a normal conducting copper alloy; h is Planck's constant; k_B is Boltzmann's constant. The above equation indicates that K_n^{-1} is influenced only by electrons in the normal conducting matrix phase. K_n^{-1} for the copper matrix phase is roughly estimated to be about 4.5 nm at 4.2 K by using the v_n value ($\simeq 1.57 \times 10^6$ msec^{-1}) [16] of pure copper. The K_n^{-1} value indicates that the high T_c values, as those of pure lead and lead–bismuth phases caused by the proximity effect, can be achieved in the dispersed state in which the interparticle distance is equal to and below about 9.0 nm. As shown in Table I, the interparticle distance is 20 to 500 nm for the copper-based alloys. The criterion of the leak distance for the appearance of high T_c is not satisfied for the rapidly quenched copper-based alloys including lead or lead–bismuth particles.

In order to achieve a superconductivity exhibiting a high T_c similar to that of the superconducting particle itself, the superconducting phase is also required to have an appropriate particle size which varies by the ratio of l to the BCS coherence length of the copper-based matrix phase (ξ). For example, in the case of $L = l/\xi = 1$, the critical radius of lead or lead–bismuth particles (r_c) for the proximity effect has been reported [17] to be above $2.965\xi_0^*$, where ξ_0^* is the coherence length of lead or lead–bismuth particles. Since the ξ_0^* value has been reported to be 83 nm for pure lead [18] and 23 nm for $Pb_{80}Bi_{20}$ [19], r_c is estimated to be about 250 nm for lead and about 70 nm for $Pb_{60}Bi_{40}$, if one assumes that the ξ_0^* value of $Pb_{60}Bi_{40}$ particles is nearly the same as that of $Pb_{80}Bi_{20}$ alloys. This estimation indicates that the radius of lead and $Pb_{60}Bi_{40}$ particles must be larger than about 250 and 70 nm, respectively, in the case of $L = l/\xi = 1$ for achieving a superconductivity by the proximity effect, in addition to the criterion of the leak distance. As shown in Table I, the observed particle radius is about 30 to 130 nm for lead and about 30 to 60 nm for ε(Pb–Bi) and/or X(Pb–Bi), which are much smaller than the critical radius for achieving superconductivity by the proximity effect. Furthermore, the actual L ($= l/\xi$) values for the present copper-based alloys with large l values is thought to be much larger than the above hypothetical value ($L = 1$) and is roughly estimated to be of the order 100 to 1000. The variation of normalized transition temperature (T_c/T_{cl}) as a function of r/ξ_0^* has theoretically been given [20, 21] for the alloy containing superconducting spherical particles in the cases of different l/ξ values as shown in Fig. 11. Here T_{cl} is the superconducting critical temperature

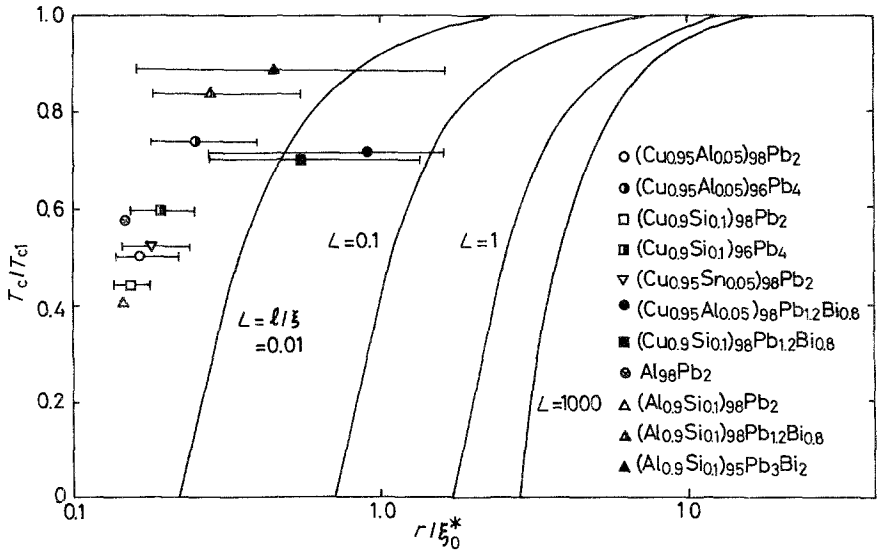

Figure 11 Theoretically estimated T_c/T_{c1} values as a function of r/ξ_0^* for rapidly quenched $(Cu_{0.95}Al_{0.05})_{100-x}Pb_x$, $(Cu_{0.9}Si_{0.1})_{100-x}Pb_x$, $(Cu_{0.95}Sn_{0.05})_{100-x}Pb_x$, $(Cu_{0.95}Al_{0.05})_{100-x}(Pb_{0.6}Bi_{0.4})_x$ and $(Cu_{0.9}Si_{0.1})_{100-x}(Pb_{0.6}Bi_{0.4})_x$ (x = 2 and 4 at%) alloys possessing the coexistent Cu(Al, Si or Sn) solid solution and lead or hcp ε(Pb–Bi) + bct X(Pb–Bi). Open and closed marks represent the average r/ξ_0^* values of their copper-based alloys. The data for rapidly quenched Al–Pb, Al–Si–Pb, Al–Si–Pb–Bi alloys are also shown for comparison.

of lead metal or the $Pb_{60}Bi_{40}$ alloy itself. The T_c/T_{c1} values expected theoretically from the particle size for the copper-based alloys are zero for $L = l/\xi$ = 1, 10 and 100, as plotted in Fig. 11. This indicates that superconductivity by the proximity effect is not obtainable for the present copper-based alloys because of the very small sizes of lead and lead–bismuth particles as well as the large interparticle distance.

Nevertheless, as summarized in Table I, the present copper-based alloys exhibited a distinct superconductivity, even though T_c values are lower by about 30 to 55% than those of lead metal and $Pb_{60}Bi_{40}$ alloys. The result is inconsistent with the expectation derived from the theory of the proximity effect. The inconsistency allows us to conclude that the appearance of superconductivity for the present copper-based alloys is not due to the proximity effect of lead or lead–bismuth particles. As a remaining mechanism for the superconductivity of the copper-based alloys, the formation of a percolation path due to the lead or lead–bismuth phase may be considered. Although it is very difficult to obtain distinct evidence of the percolation circuit, it was revealed in Figs 2 and 4 that (i) lead and lead–bismuth particles tend to precipitate on the grain boundaries, sub-boundaries and dislocations, and (ii) their particles precipitate very densely even within the matrix. Such a precipitation mode of the superconducting particles might allow us to infer the formation of a superconducting circuit, even though the total volume fraction of the lead or lead–bismuth phase is not large enough to form a homogeneous percolation circuit over the whole area within each grain. Accordingly, the reason why the rapidly quenched copper-based alloys including lead or lead–bismuth particles exhibited high T_c values, in spite of the smaller particle size and the larger interparticle distance as compared with the critical values for superconductivity by the proximity effect, is thought to originate from the formation of a superconducting lead or lead–bismuth percolation path on the grain boundaries, sub-boundaries and/or tangled dislocations.

5. Summary

Copper-based alloys exhibiting superconductivity were produced by rapid quenching the $(Cu_{0.95}Al_{0.05})_{100-x}Pb_x$, $(Cu_{0.9}Si_{0.1})_{100-x}Pb_x$, $(Cu_{0.95}Sn_{0.05})_{100-x}Pb_x$ (x = 1, 2 and 4 at%), $(Cu_{0.95}Al_{0.05})_{98}Pb_{1.2}Bi_{0.8}$ and $(Cu_{0.9}Si_{0.1})_{98}Pb_{1.2}Bi_{0.8}$ alloys with immiscible lead and bismuth elements. The rapidly quenched alloys are composed of copper solid solution containing aluminium, silicon or tin and lead or hcp ε(Pb–Bi + bct X(Pb–Bi) particles. The particle size and interparticle distance (D) within the grains are, respectively, about 30 to 130 and 20 to 200 nm for lead, and about 30 to 60 and 30 to 150 nm for lead–bismuth, but the D value at the grain boundaries is much smaller. The formation of the copper-based alloys including finely dispersed lead or lead–bismuth particles was limited to less than about 5 at% Pb or ε(Pb + Bi). The mechanism of the appearance of superconductivity for the copper-based alloys was inferred to be due to the formation of a superconducting lead or lead–bismuth percolation path on the grain boundaries, sub-boundaries and/or dislocations, rather than to the proximity effect of lead and lead–bismuth particles. T_c was in the range from 3.2 to 5.5 K for the Cu–M–Pb (M = aluminium, silicon or tin) alloys and from 6.2 to 6.3 K for Cu–M–Pb–Bi (M = aluminium, silicon or tin) alloys. The temperature gradient of H_{c2} near T_c and the H_{c2} value at 4.2 K are 0.23 to 0.30 TK^{-1} and 0.47 to 0.93 T for the Cu–M–Pb–Bi (M = aluminium or silicon) alloys. J_c is about 1.1×10^5 to 2.7×10^5 Am^{-2} at $H = 0$ and 4.21 K and the maximum fluxoid pinning force is about 1.1×10^4 Nm^{-3} at 4.21 K. Thus, the application of the rapid-quenching technique to the copper-based alloys containing immiscible lead or lead + bismuth elements was found to be very useful for the production of superconducting copper-based alloys including fine lead or lead–bismuth particles.

References

1. H. A. DAVIES, in "Amorphous Metallic Alloys", edited by F. E. Luborsky (Butterworth, London, 1983) p. 8.
2. A. INOUE, M. OGUCHI, K. MATSUZAKI, Y. HARAKAWA and T. MASUMOTO, *J. Mater. Sci.* **21** (1986) 260.
3. A. INOUE, M. OGUCHI, K. MATSUZAKI and T. MASUMOTO, *Int. J. Rapid Solidification* **1** (1984–5) 273.
4. K. MATSUZAKI, A. INOUE, M. OGUCHI and T. MASUMOTO, *Int. J. Rapid Solidification* **2** (1986–7) in press.

5. A. INOUE, N. YANO, K. MATSUZAKI and T. MASUMOTO, *J. Mater. Sci.* **22** (1987) 123.
6. A. INOUE, M. OGUCHI, K. MATSUZAKI and T. MASUMOTO, *Int. J. Rapid Solidification* **2** (1986–7) in press.
7. A. INOUE, T. OGASHIWA, K. MATSUZAKI and T. MASUMOTO, *J. Mater. Sci.* **22** (1987) in press.
8. M. HANSEN, "Constitution of Binary Alloys" (McGraw-Hill, New York, 1958) pp 84, 629, 633.
9. W. B. PEARSON, "Handbook of Lattice Spacings and Structures of Metals and Alloys" (Pergamon, London, 1958) p. 803.
10. D. SOLOMON and W. MORRIS-JONES, *Phil. Mag.* **11** (1931) 1090.
11. H. HOFE and H. HANEMANN, *Z. Metallkunde* **32** (1940) 112.
12. C. SURYANARAYANA and T. R. ANANTHARAMAN, *Solid State Commun.* **12** (1973) 87.
13. I. LIVINGSTON, *Phys. Rev.* **129** (1963) 1943.
14. T. OTSUKA, in "Ferroelectrics and Superconductors", edited by K. Adachi (Japan Institute of Metals, Sendai, 1973) p. 131.
15. G. DEUTSCHER and D. G. DE GENNES, in "Superconductivity" Vol. 2, edited by R. D. Parks (Marcel Dekker, New York, 1969) p. 1005.
16. C. KITTEL, "Introduction to Solid State Physics", 5th edn. (John Wiley, New York, 1976) p. 154.
17. W. SILVERT and A. SINGH, *Phys. Rev. Lett.* **28** (1972) 222.
18. C. KITTEL, *Solid State Physics* (John Wiley, New York, 1976) p. 376.
19. M. LYON and G. ZEPP, *Can. J. Phys.* **55** (1977) 55.
20. W. SILVERT, *Solid State Commun.* **14** (1974) 635.
21. W. SILVERT and L. N. COOPER, *Phys. Rev.* **141** (1966) 336.

Received 14 July
and accepted 22 September 1986